Electronic Supplementary Information

Encapsulating Surface-Clean Metal Nanoparticles inside Metal-Organic Frameworks for Enhanced Catalysis using a Novel γ-Ray Radiation Approach

Zhen Zhang,[a] Xiaoling Cui,[a] Wei Yuan,[a] Qihao Yang,[b] Huarong Liu,[a] Hangxun Xu*[a] and Hai-Long Jiang*[b]*

[a] CAS Key Laboratory of Soft Matter Chemistry, Department of Polymer Science and Engineering, University of Science and Technology of China, Hefei, Anhui 230026, P. R. China.

[b] CAS Key Laboratory of Soft Matter Chemistry, Hefei National Laboratory for Physical Sciences at the Microscale, Department of Chemistry, University of Science and Technology of China, Hefei, Anhui 230026, P. R. China.

*To whom correspondence should be addressed.

E-mail: hrliu@ustc.edu.cn (H.L.); hxu@ustc.edu.cn (H.X.); jianglab@ustc.edu.cn (H.-L.J.)

Table S1 Experimental conditions for the preparation of M@UiO-66-NH_2/R by γ-ray radiation reduction.[a]

Sample	Precursor	Concentration of precursor (M)	Dose rate (Gy/min)	Absorbed Dose (kGy)
1	K_2PdCl_4	0.005	100	6
2			100	18
3			100	36
4			25	18
5	K_2PdCl_4	0.002	100	18
6	K_2PdCl_4	0.010	100	18
7	K_2PtCl_4	0.005	100	18
8	$KAuCl_4$	0.005	100	18

[a] Other conditions: 50 mg of UiO-66-NH_2, 5 mL of deionized water, and 0.2 mL of isopropyl alcohol were used.

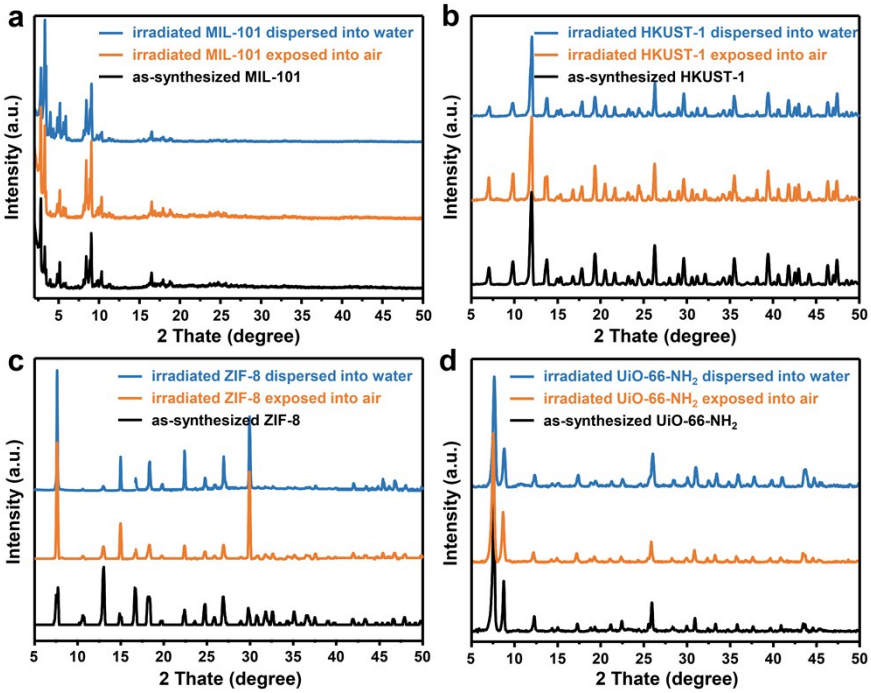

Fig. S1 PXRD patterns of (a) HKUST-1 before and after γ-ray radiation, (b) MIL-101 before and after γ-ray radiation, (c) ZIF-8 before and after γ-ray radiation, and (d) UiO-66-NH_2 before and after γ-ray radiation (The MOFs samples were dispersed into water or exposed into air and irradiated with an absorbed dose of 36 kGy at a dose rate of 100 Gy/min).

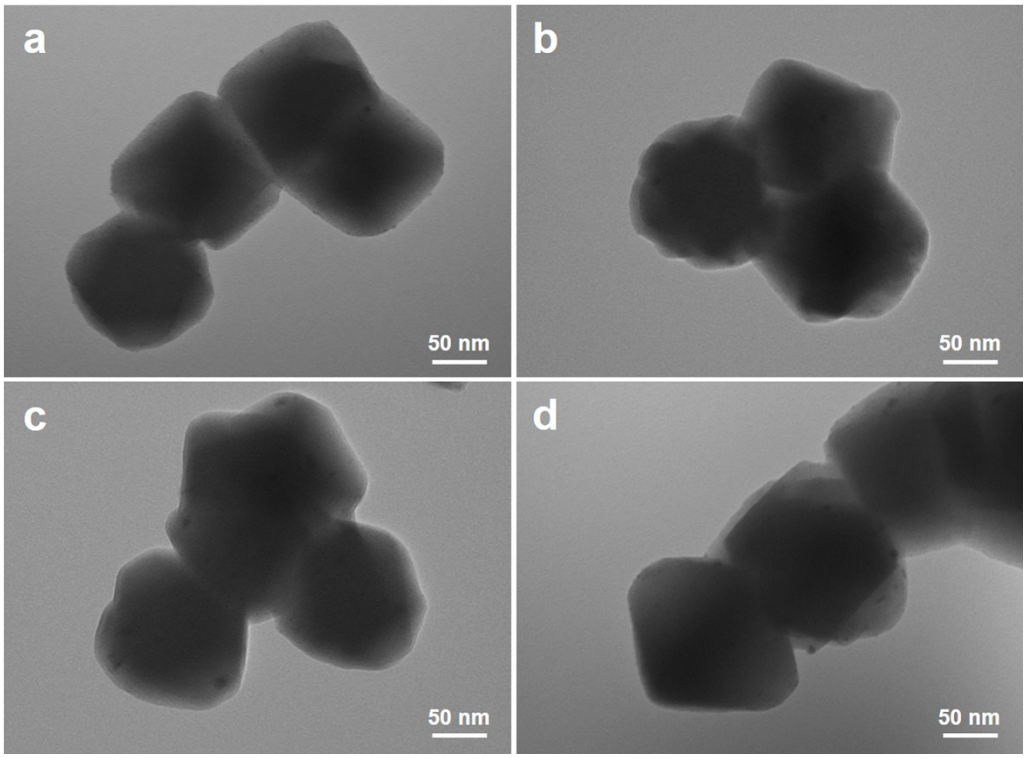

Fig. S2 TEM images of Pd@UiO-66-NH_2/R synthesized by γ-ray radiation with different absorbed doses and/or dose rates: (a) 6 kGy and 100 Gy/min; (b) 18 kGy and 100 Gy/min; (c) 36 kGy and 100 Gy/min; (d) 18 kGy and 25 Gy/min.

Table S2 Pd@UiO-66-NH_2/R synthesized under different absorbed doses and/or dose rates.

Sample	**Dose rate**	**Absorbed dose**	**Pd content** (wt %)		**Loading efficiency** (%)
			Theoretical value	**ICP-MS result**	
1	100 Gy/min	6 kGy	5.34	0.89	16.7
2	100 Gy/min	18 kGy		3.55	66.5
3	100 Gy/min	36 kGy		4.06	76.0
4	25 Gy/min	18 kGy		3.84	71.8

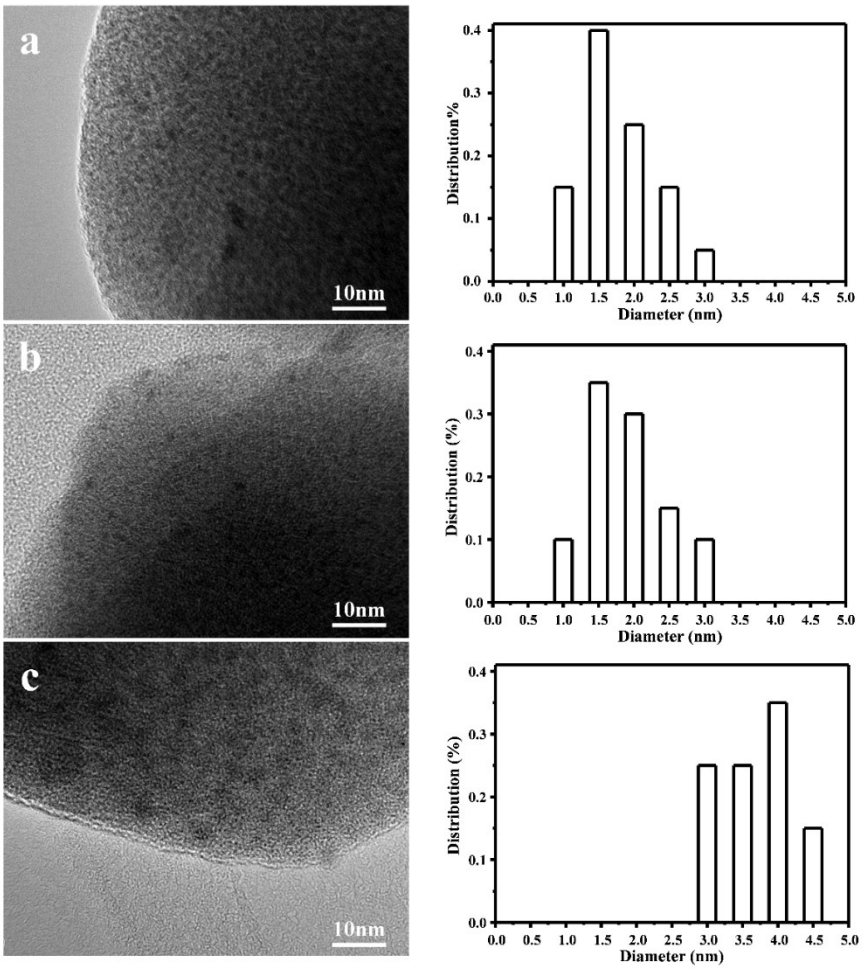

Fig. S3 TEM images of Pd@UiO-66-NH_2/R and the histograms of the size distribution of the corresponding Pd NCs synthesized by γ-radiation of UiO-66-NH_2 impregnated with different concentrations of K_2PdCl_4: (a) 0.002 M, (b) 0.005 M, and (c) 0.010 M.

Table S3 Metal contents and corresponding diameters of various metal NPs@UiO-66-NH_2.

Sample	Metal content (wt%)			Loading efficiency (%)	Diameter of metal NCs[c] (nm)
	Theoretical value	ICP-MS result	XPS data		
2 (Pd)	5.34	3.55	0.43	66.5	1.9
5 (Pd)	2.16	1.52	0.24	70.4	1.7
6 (Pd)	10.69	6.90	1.07	64.5	3.7
9[a] (Pd)	5.34	2.12	0.54	39.7	2.9
10[b] (Pd)	5.34	2.35	0.44	44.0	3.3
7 (Pt)	9.78	5.48	-	56.0	1.1
8 (Au)	9.91	7.48	-	75.5	1.0

[a]The synthetic condition was the same as the sample 2 but H_2 reduction was used in the synthesis instead of using γ-ray radiation.

[b]The synthetic condition was the same as the sample 2 but $NaBH_4$ reduction was used in the synthesis instead of using γ-ray radiation.

[c]The average particle diameter was measured from 100 particles in the HRTEM images.

Table S4 BET surface area and pore volume of M@UiO-66-NH_2 and 3.55 wt% Pd@UiO-66-NH_2/R after cycling tests.

Sample	BET ($m^2 g^{-1}$)	Pore Volume ($cm^3 g^{-1}$)
UiO-66-NH_2	1126.2	0.46
1 (Pd)	782.4	0.31
2 (Pd)	750.6	0.30
2 (Pd) after cycling tests	687.9	0.29
9 (Pd)	608.1	0.22
10 (Pd)	584.8	0.21
7 (Pt)	708.2	0.41
8 (Au)	677.4	0.29

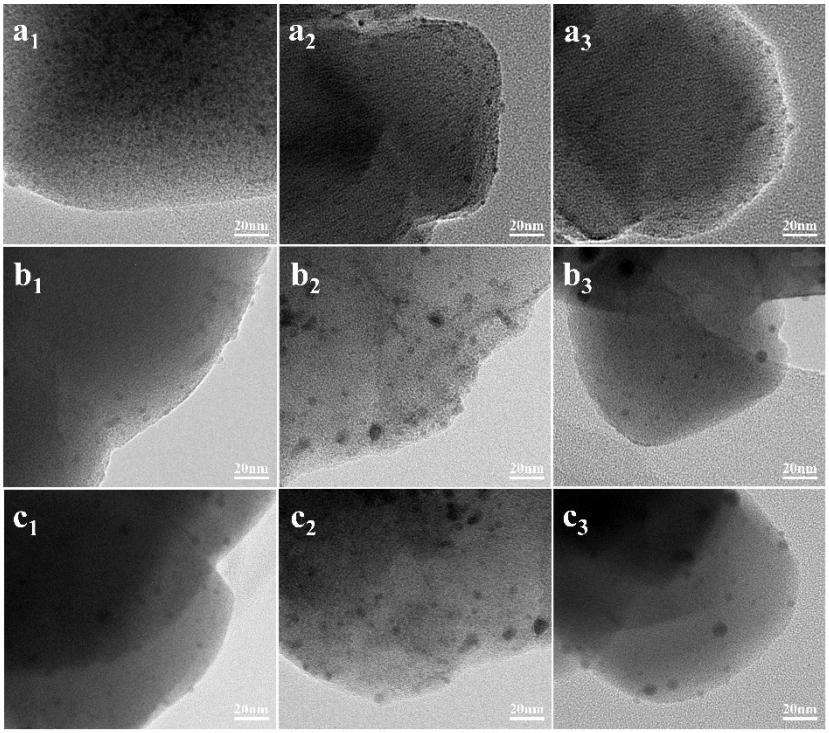

Fig. S4 TEM images of (a_{1-3}) Pd@UiO-66-NH_2/R (3.55 wt% Pd), (b_{1-3}) Pd@UiO-66-NH_2/H, and (c_{1-3}) Pd@UiO-66-NH_2/B: (a_1, b_1, c_1) as-synthesized samples, (a_2, b_2, c_2) after five cycles of catalytic tests, (a_3, b_3, c_3) after calcination in air at 250 °C for 2 h.

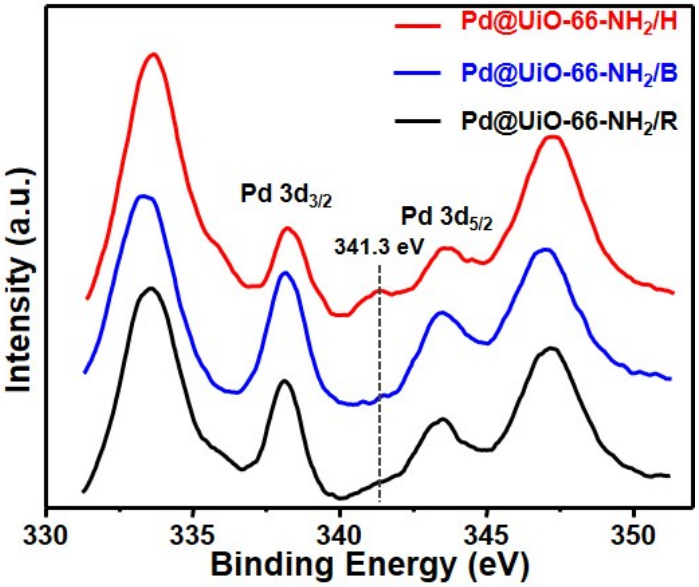

Fig. S5 XPS spectra of Pd@UiO-66-NH_2/R (3.55 wt% Pd), Pd@UiO-66-NH_2/H, and Pd@UiO-66-NH_2/B.

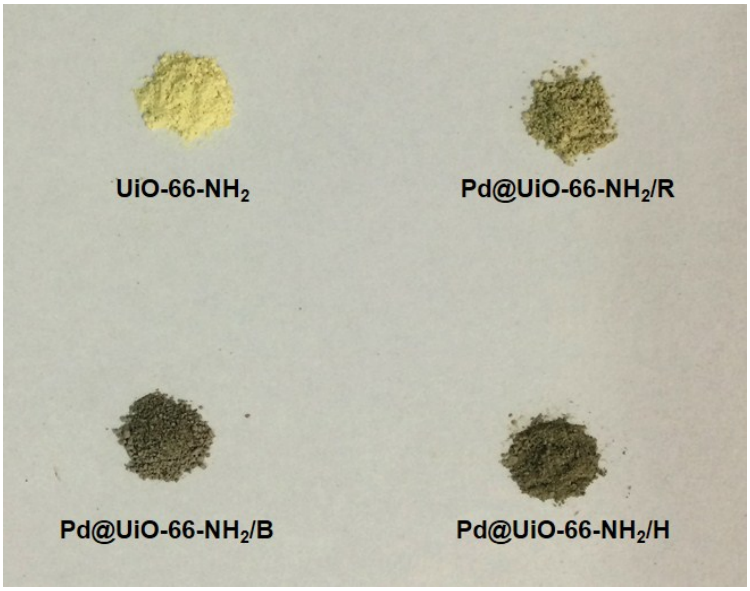

Fig. S6 Digital photographs of as-synthesized UiO-66-NH_2, Pd@UiO-66-NH_2/R (3.55 wt% Pd), Pd@UiO-66-NH_2/B, and Pd@UiO-66-NH_2/H.

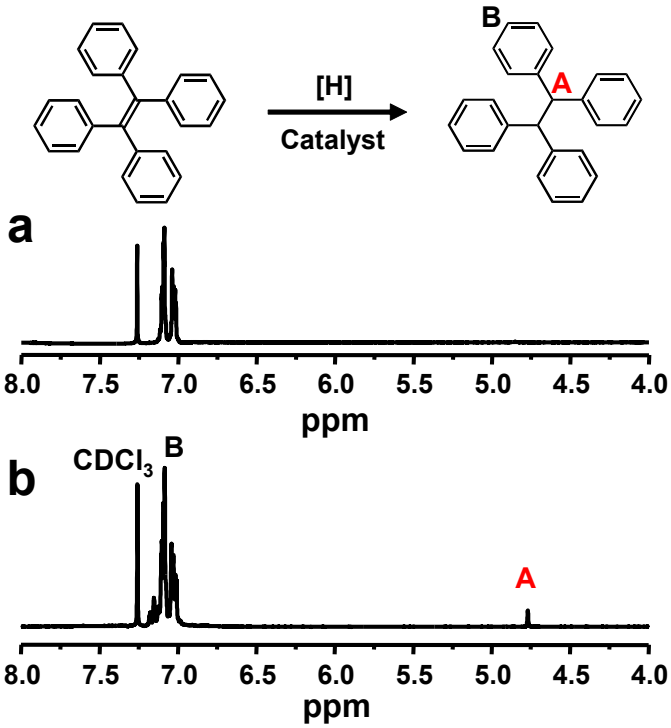

Fig. S7 ^{1}H NMR spectra of products obtained after the hydrogenation reaction of tetraphenylethylene using different catalysts: (a) Pd@UiO-66-NH_2/R (3.55 wt% Pd) and (b) Pd/C. The absence of the corresponding peak around 4.7 ppm clearly indicates that the hydrogenation reaction could not occur using Pd@UiO-66-NH_2/R.

Table S5 Summary of the performance of the recently reported catalysts for the hydrogenation of styrene.

Catalyst	**TOF** (min^{-1})	**Ref**
Pd@MOF-3	0.234	Inorg. Chem., 2016, 55, 2345
Pd/MOF-5	0.212	J. Mater. Chem., 2007, 17, 3827
Pd/MIL-101	1.094	Chem. Commun., 2008, 35, 4192
Pd/UiO-66	0.588	Angew. Chem. Int. Ed., 2016, 55, 7379
Pd/UiO-66@PDMS-60	2.308	
Ni@MesMOF	0.796	Chem. Commun., 2010, 46, 3086
Pd/C	0.50	This work
1.52 wt% Pd@UiO-66-NH_2/R	2.222	This work
3.55 wt% Pd@UiO-66-NH_2/R	2.0	This work
6.90 wt% Pd@UiO-66-NH_2/R	1.429	This work
Pd@UiO-66-NH_2/B	0.714	This work
Pd@UiO-66-NH_2/H	0.769	This work

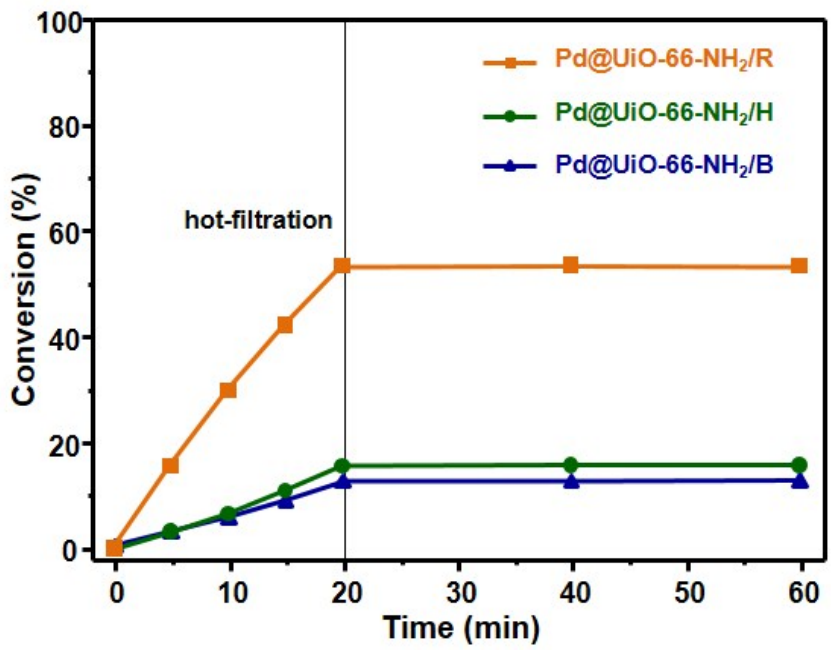

Fig. S8 Hot-filtration tests for the catalytic hydrogenation of styrene over Pd@UiO-66-NH_2 catalysts synthesized via different reduction methods (the molar ratio of Pd:styrene = 1:100).

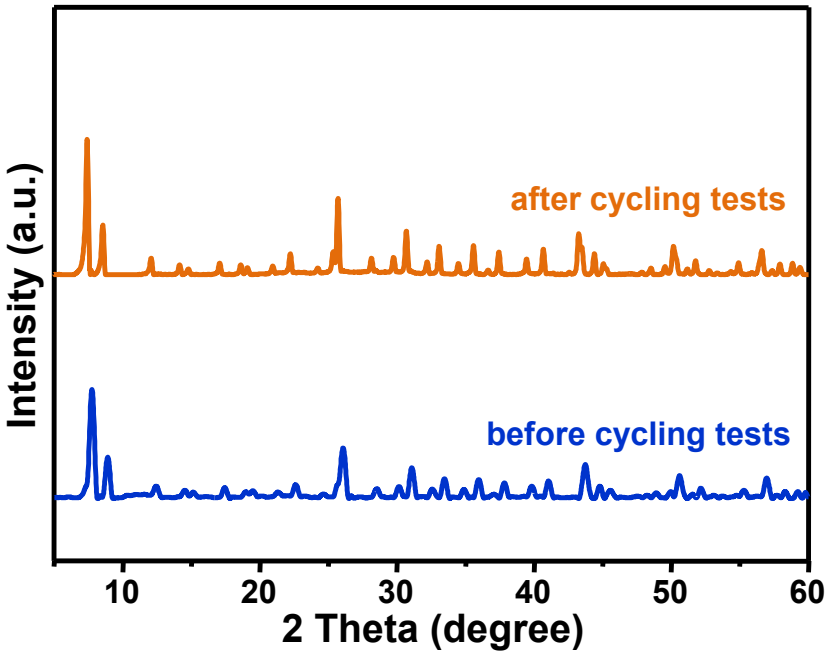

Fig. S9 PXRD patterns of Pd@UiO-66-NH_2/R (3.55 wt% Pd) before and after five cycling tests.

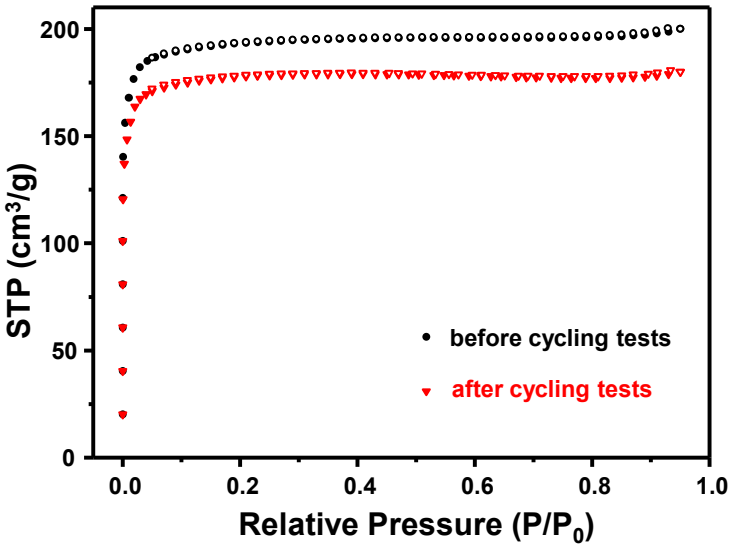

Fig. S10 Nitrogen adsorption and desorption isotherms of UiO-66-NH_2/R (3.55 wt% Pd) before and after five cycling tests.

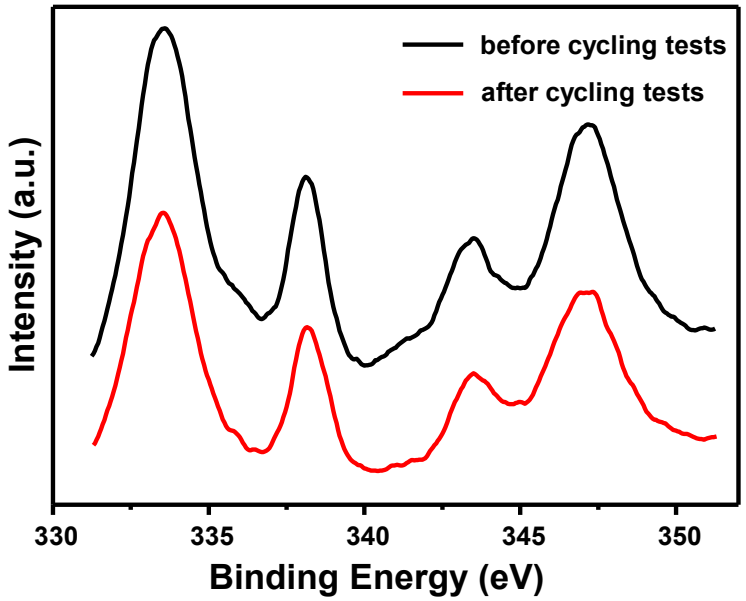

Fig. S11 XPS spectra of Pd@UiO-66-NH_2/R (3.55 wt% Pd) before and after five cycling tests.

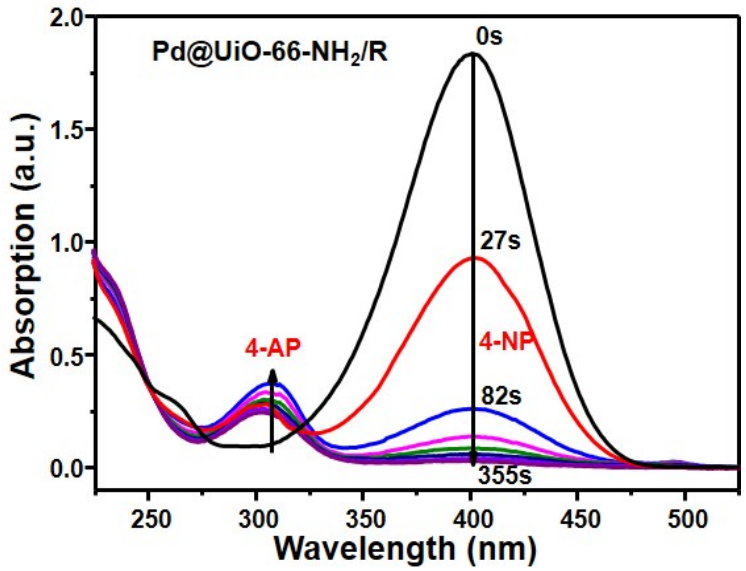

Fig. S12 UV-Vis absorption spectra recording the reduction process of 4-nitrophenol completed in 355 s for Pd@UiO-66-NH_2/R (3.55 wt% Pd).

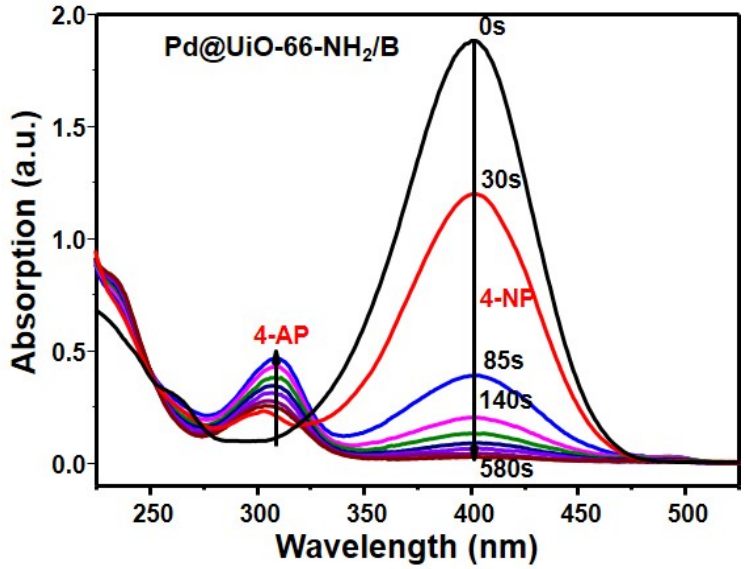

Fig. S13 UV-Vis absorption spectra recording the reduction process of 4-nitrophenol completed in 580 s for Pd@UiO-66-NH_2/B.

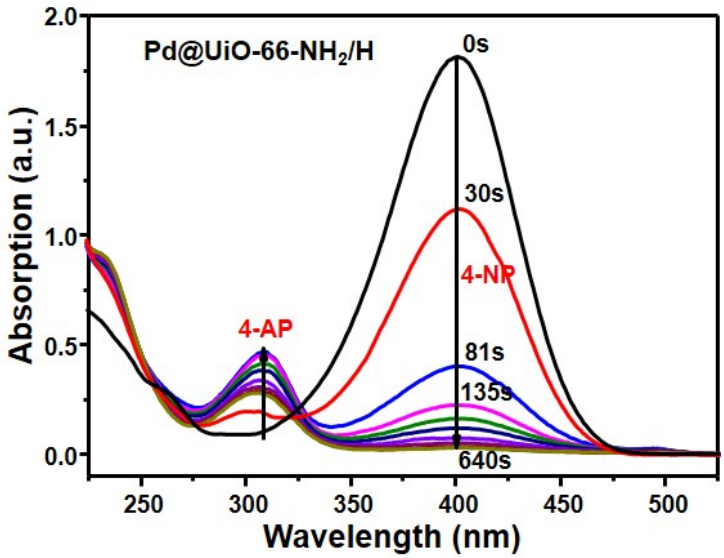

Fig. S14 UV-Vis absorption spectra recording the reduction process of 4-nitrophenol completed in 640 s for Pd@UiO-66-NH_2/H.

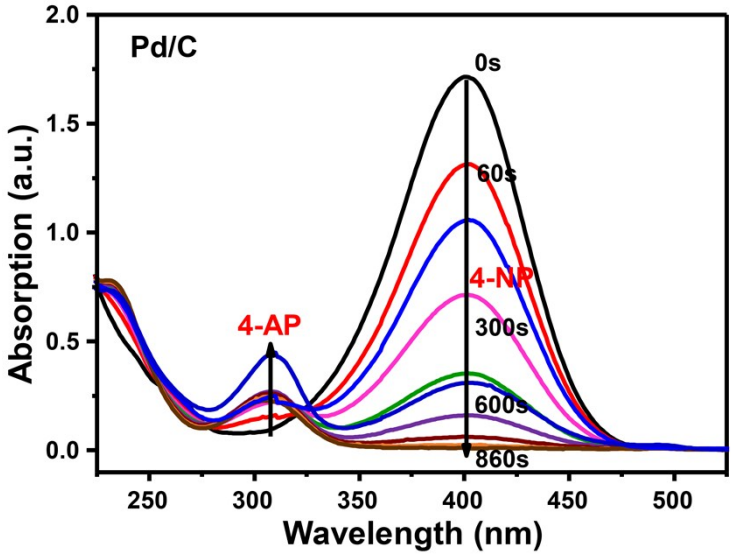

Fig. S15 UV-Vis absorption spectra recording the reduction process of 4-nitrophenol completed in 860 s for Pd/C catalyst.

Table S6 Summary of the performance of the recently reported Pd-based catalysts for reduction of 4-nitrophenol.

Catalyst	**Kinetic constant** k_{app} (min^{-1})	**Ref**
Fe_3O_4@TiO_2/Au@SiO_2/Pd	0.23887	Chem. Commun., 2013, 49, 7596
Pd@Au core–shell nanotetrapod	0.139	Nanoscale, 2014, 6, 9273
Pd/C	0.5298	Nanoscale, 2013, 5, 1843
Pd/SBA15	0.708	J. Supercrit. Fluids, 2011, 56, 213
Pd@MIL-101	0.1137	Funct. Mater. Let., 2012, 5, 1250039
Pd/Magnetic porous carbon	0.72	J. Mater. Chem. A, 2014, 2, 18775
Pd@MIL-88B	1.09	RSC Adv., 2015, 5, 46583
Pd@UiO-66-NH_2/R	1.455	This work
Pd@UiO-66-NH_2/B	1.126	This work
Pd@UiO-66-NH_2/H	1.123	This work
Pd/C	0.341	This work

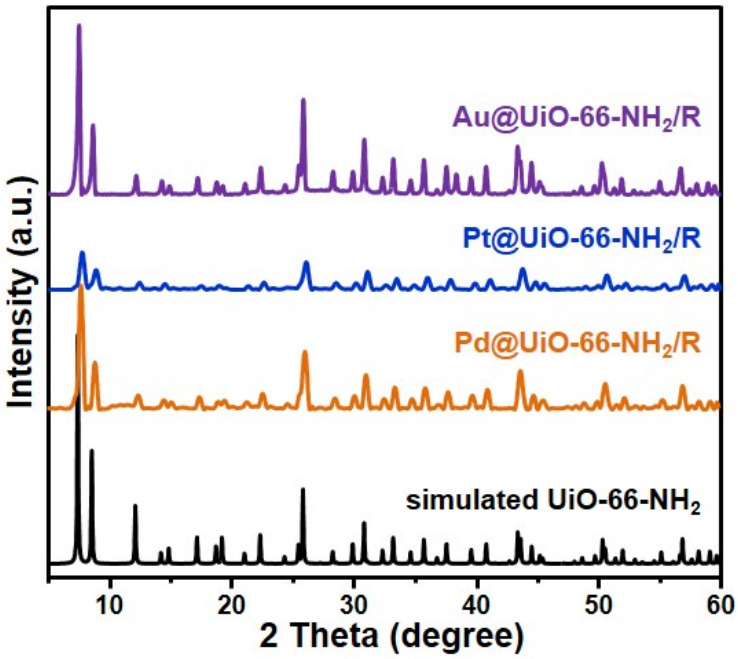

Fig. S16 PXRD patterns of simulated UiO-66-NH_2, Pd@UiO-66-NH_2/R, Pt@UiO-66-NH_2/R, and Au@UiO-66-NH_2/R.

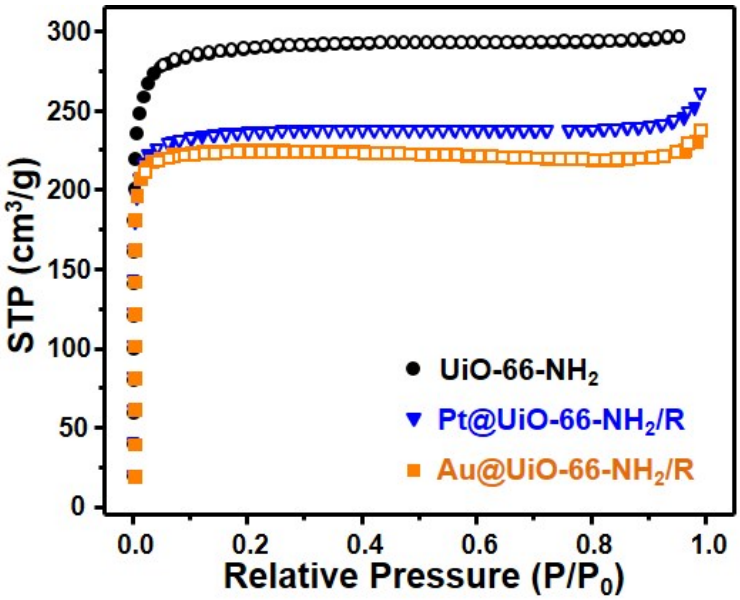

Fig. S17 The nitrogen adsorption and desorption isotherms of UiO-66-NH_2, Pt@UiO-66-NH_2/R, and Au@UiO-66-NH_2/R.

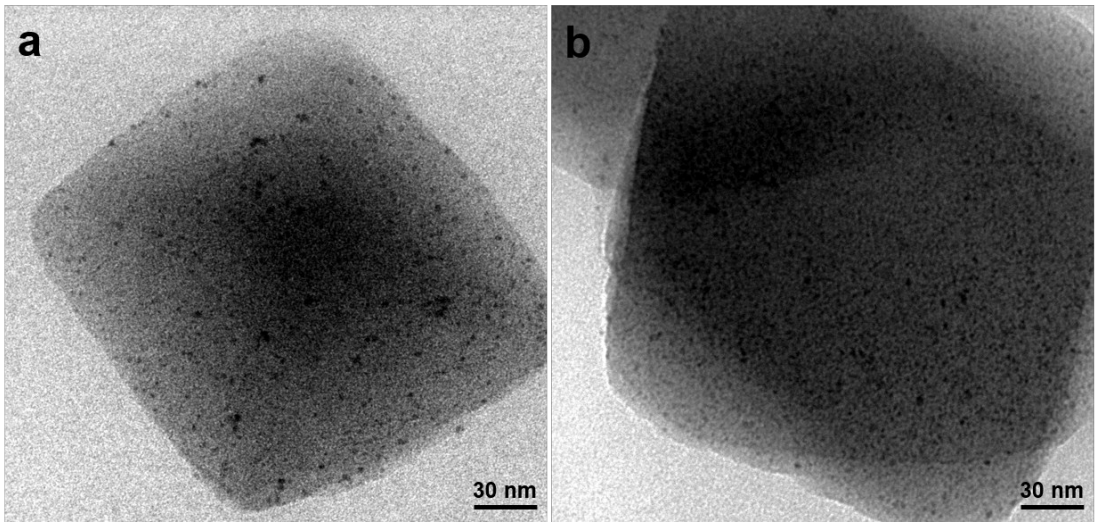

Fig. S18 TEM images of (a) Pd@MIL-101/R with an average diameter of ~1.9 nm and (b) Pt@MIL-101/R with an average diameter of ~1.7 nm synthesized through γ-ray radiation method.

The synthesis procedure of Pd@MIL-101/R is identical with Pd@UiO-66-NH_2/R (see experimental section for details) except UiO-66-NH_2 was replaced by 50 mg of activated MIL-101. The same procedure was also used to synthesize Pt@MIL-101/R. In this case, 5 mL K_2PtCl_4 aqueous solution (0.005 M) was used (Table S1).